



THE UNIVERSITY *of* EDINBURGH

Edinburgh Research Explorer

## Contact Resistance Heating of Unidirectional Carbon Fibre Tows in a Powder-Epoxy Towpregging Line

**Citation for published version:**

Celik, M, Noble, T, Haseeb, A, Maguire, J, Robert, C & Ó Brádaigh, CM 2022, 'Contact Resistance Heating of Unidirectional Carbon Fibre Tows in a Powder-Epoxy Towpregging Line', *Plastics, Rubber and Composites*. <https://doi.org/10.1080/14658011.2022.2108982>

**Digital Object Identifier (DOI):**

[10.1080/14658011.2022.2108982](https://doi.org/10.1080/14658011.2022.2108982)

**Link:**

[Link to publication record in Edinburgh Research Explorer](#)

**Document Version:**

Peer reviewed version

**Published In:**

Plastics, Rubber and Composites

**General rights**

Copyright for the publications made accessible via the Edinburgh Research Explorer is retained by the author(s) and / or other copyright owners and it is a condition of accessing these publications that users recognise and abide by the legal requirements associated with these rights.

**Take down policy**

The University of Edinburgh has made every reasonable effort to ensure that Edinburgh Research Explorer content complies with UK legislation. If you believe that the public display of this file breaches copyright please contact [openaccess@ed.ac.uk](mailto:openaccess@ed.ac.uk) providing details, and we will remove access to the work immediately and investigate your claim.



# Contact Resistance Heating of Unidirectional Carbon Fibre Tows in a Powder-Epoxy Towpregging Line

Murat Çelik<sup>1</sup>, Thomas Noble<sup>1</sup>, Abdul Haseeb<sup>1</sup>, James Maguire<sup>1</sup>, Colin Robert<sup>1</sup>,  
Conchúr M. Ó Brádaigh<sup>1</sup>

<sup>1</sup>School of Engineering, Institute for Materials and Processes, The University of Edinburgh,  
Sanderson Building, King's Buildings, Edinburgh, EH9 3FB, UK

**Keywords:** *Joule heating, contact resistance, contact resistance heating, towpreg, powder epoxy*

## Abstract

Joule heating is a promising heating method used in the composites industry, which is characterised by high heating efficiencies and low power consumption. However, imperfect contact at the electrode/material interfaces results in contact resistances. Contact resistances play a major role in Joule heating systems, therefore, identifying contact resistances provides a better understanding of the heating process. Furthermore, the accuracy of the process models of heating systems can be increased by taking contact resistances into account. In this study, contact resistances of the Joule heating section in a powder-epoxy based towpregging line were explored. For different process parameters, such as production speed, tension and temperature, contact resistances occurring between metal roller electrodes and dry carbon fibre tows (i.e. without powder-epoxy) were measured to gain an insight into the heating process. Moreover, the effect of contact resistance heating on the overall temperature profile of the carbon fibre tows was determined with an infrared thermal camera. A simplified finite element model was developed to calculate the temperature distribution along the moving carbon fibre tow, which showed a good agreement with the experimental data. Results suggest that contact resistances in the towpregging line were significant and contact resistance heating changed the heating profile.

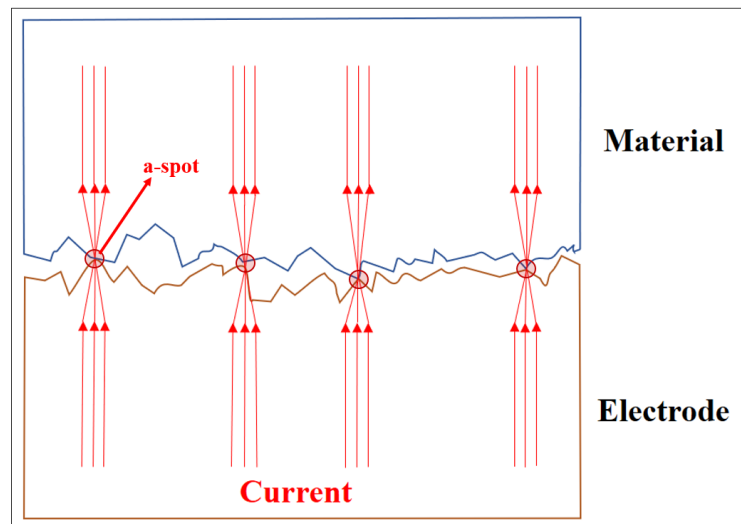
## 1. Introduction

Current passing through electrically conductive fibres generates heat due to the resistance of the fibres, which is known as the Joule effect. Joule heating, or resistive heating, is a practical heating technique used in the composite industry, and can be used as a heating method in curing [1]–[7] or self-healing [8]–[11] applications. When compared to conventional heating systems (infrared, induction, convection oven etc.), the heating efficiency of Joule heating systems is excellent, as the energy losses are minimal due to the intrinsic origin of Joule heating, coming from within the fibres. This advantage leads to significant power consumption reduction, compared to other power sources such as oven heating and autoclave [12]. Mas et al. [3] demonstrated the substantial difference in the power requirements of Joule heating and oven heating for carbon nanotube (CNT) based polymer composites (up to 99.5% reduction compared

43 to oven heating). For the same material volume, the oven power operated at 800 W, while the  
44 Joule heating set up only consumed a power of 4 W for the curing of CNT based composite.  
45 Furthermore, since the heat loss is minimal and heat generation takes place in the fibres, Joule  
46 heating is rapid and uniform; with high temperatures ( $>100^{\circ}\text{C}$ ) being achieved within seconds  
47 [13].

48  
49 The composite and electrode interface has a pivotal role in Joule heating systems. While carbon  
50 fibres are electrically conductive, the polymer matrix is not, therefore the contact between the  
51 composite and the electrode surface is discontinuous. Furthermore, micron-size asperities on  
52 the electrode surface aggravate the contact resistances at the interface, which constrict the  
53 current flow to the so-called “a-spots” (Figure 1) [14]. Localised heat generation is observed at  
54 the interfaces due to the contact resistances.

55



56

57 **Figure 1:** Constrained current flow due to the contact  
58 resistances, inspired by Hamedi and Atashparva [15]

59  
60 The contact resistance heating term [16], [17] is used to define the heat generation by the contact  
61 resistances at the electrode-material interfaces. Depending on the electrode type, contact  
62 resistance heating can be significant, especially for prolonged times of current supply [16].  
63 Contact resistance is a complex phenomenon, reducing the Joule heating efficiency and creating  
64 thermal gradients, and is influenced by a variety of different parameters, including actual contact  
65 area, applied pressure, and surface roughness. Kwok and Hahn [9] investigated various  
66 electrode types for a Joule heating system used on a carbon fibre-based composite, and  
67 quantified contact resistance values for different electrode-composite couplings. They  
68 illustrated that the contact resistance values can be surprisingly dissimilar depending on the  
69 electrode. For the same material, the large contact intermediate electrode, which clamps a  
70 conductive rubber pad to the material to increase the contact area, had a contact resistance value  
71 of  $0.788\ \Omega$ , while it was  $24.78\ \Omega$  when the alligator clips are attached to the bare composite (no  
72 intermediate electrodes). It was also observed that contact resistances lead to spikes in the  
73 temperature field, creating non-uniformity in the heating zone. Similar thermal gradients due to

74 the non-uniform temperature profile caused by contact resistances were reported by Zantout and  
75 Zhupanska [14] with the help of a numerical model validated by experimental data. The contact  
76 resistance of the composite/electrode interfaces can also be reduced by improving the contact  
77 between the conductive fibres and electrode surface, such as sanding the composite surface to  
78 expose carbon fibres [18].

79  
80 Recently, a powder-epoxy based towpregging line has been developed by Robert et al. [19]. The  
81 towpregging line deposits powder-epoxy on carbon fibre tows, melts the powder-epoxy using  
82 Joule heating, and then consolidates molten powder-epoxy within the carbon fibre tow to  
83 produce semi-impregnated towpregs. This can be achieved due to the advantages of powder-  
84 epoxy, such as separated melting/curing temperatures and low resin viscosity [20], [21]. A  
85 detailed description of the system was given in [19], [22]. The use of Joule heating within the  
86 towpregging line necessitates the identification of contact resistances in the system. In doing  
87 so, the overall heating process can be better understood, as the non-uniformities and thermal  
88 gradient of the heating affect the powder melting characteristics. Furthermore, measuring the  
89 contact resistance values provides valuable input for process models of the towpregging line,  
90 which are in development concurrently, and will help to increase the model accuracy.

91  
92 In this study, the contact resistance phenomenon of the Joule heating system of the powder-  
93 epoxy based towpregging line is explored. For different process parameters of towpreg  
94 production, contact resistance values are measured with an experimental system to assess the  
95 significance of contact resistances and contact resistance heating in the production. As an initial  
96 step in order to reduce complexity, powder-epoxy was not deposited on the carbon fibre tows  
97 during the contact resistance tests presented in this paper.

## 100 2. Experimental

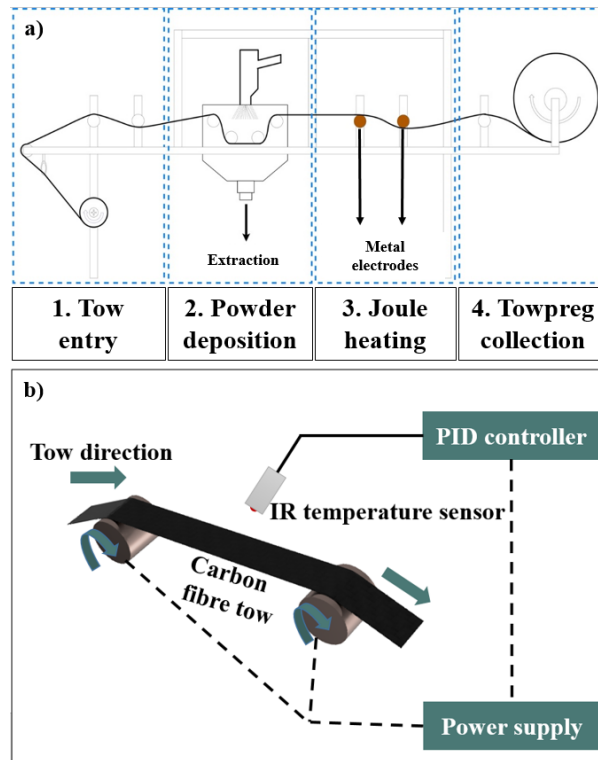
### 102 *2.1. Towpregging line and Joule heating system*

103 Robert et al. [19] developed a powder-epoxy based towpregging line that is capable of  
104 producing low-cost, high-quality versatile towpregs for automated fibre placement (AFP) or  
105 filament winding applications. Towpreg production takes place in the following steps, as shown  
106 in Figure 2a):

- 107 1. Carbon fibre tows are pulled through a series of rollers.
- 108 2. Powder-epoxy is deposited on the carbon fibre tow using electrostatic spray.
- 109 3. Joule heating is used to heat the tow and melt the powder-epoxy. Melting of the powder  
110 starts around 40°C.
- 111 4. Molten powder-epoxy consolidates and the towpreg is collected.

112

113



114

115

116

117

**Figure 2:** Overview of a) towpreg production b) Joule heating section of the towpregging line.

118

119

120

121

122

123

124

125

126

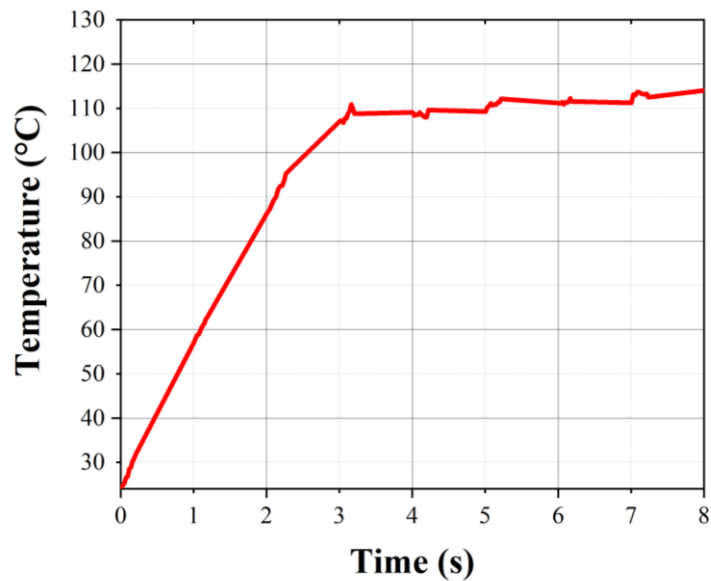
127

128

129

130

The towpregging line consists of different sensors and equipment to monitor and control the production process. PID controllers are used to adjust the tension of the tow, the speed of the production, and the temperature of the tow. A constant current (0 to 2 A, depending on the target temperature) is supplied via a power supply between two rotating metal roller electrodes in the Joule heating section as the tow travels during production, as shown in Figure 2 2b). Due to the electrically conductive nature of carbon fibre, heat is produced from the current passing through the carbon fibre tow, melting the powder-epoxy. IR temperatures constantly monitor the temperature of the tow and send data to the PID controller, which controls the power supply providing the current to the roller electrodes. According to the IR readings, the PID controller regulates the voltage supplied to reach the desired tow temperature. The temperature of the tow increases rapidly when electrical current is introduced in the Joule heating system, reaching 100°C in under 3 seconds, as illustrated in Figure 3.



131

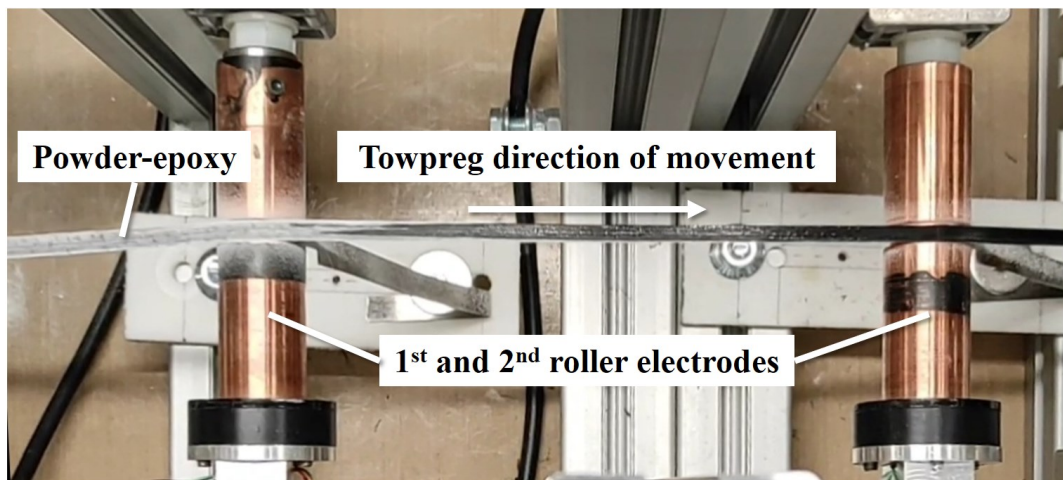
**Figure 3:** Change of maximum temperature of the moving tow when the current is supplied.

132  
133

134

135 As a result of the heat produced from the Joule heating, powder-epoxy deposited on the carbon  
 136 fibre melts and impregnates into the tow, creating the towpreg, as shown in Figure 4. Note that  
 137 this study focuses on the contact resistance heating of dry carbon fibre tows, however, the  
 138 production of towpreg with powder-epoxy is shown here to illustrate the powder melting  
 139 process. The fibre volume fraction of the towpregs can be controlled within the towpregging  
 140 line system by managing the process parameters, such as varying the production speed or  
 141 changing electrostatic spraying settings.

142



143

**Figure 4:** Top view of the Joule heating system. Powder-epoxy on the carbon fibre tow melts when an electric current is supplied.

144  
145

146

147

## 2.2. Materials

148

149

150

151

152

153

154

155

156

157

158

159

Toray T700S-24K-50C carbon fibre tow was used because of its mechanical properties [23]. The sizing weight percentage was 1%, and the tow had approximately 24,000 carbon fibre filaments. The roller electrodes were made of conductive PTFE coated stainless steel, which were electrified by the slip-rings fitted inside. According to the coating company (PTFE Applied Coatings Co.), the conductive PTFE coating was 50 microns thick, with a roughness within micrometre range. Typically, electrical conductivity is attained to the PTFE coatings with the use of anti-static additives. Usual volume resistivity values are for such coatings are in the range of 7-10 ohm.cm [24], [25]. Conductive PTFE coating was used because, during normal operation of the towpregging line, it prevents powder and fibre build-up on the surfaces. Note, however, that the experiments in this study focused on dry carbon fibre tows (i.e. powder was absent). A FLIR A655SC Infrared thermal camera was used to capture temperature distribution in the carbon fibre tow.

160

161

## 2.3. Contact resistance measurements

162

163

164

165

166

167

In the regions where the roller electrodes contact carbon fibre tows, contact resistances are present due to the imperfect contact between the electrode surface and carbon fibre tow. Because of these contact resistances, the electric current is constricted and can only be conducted through conducting spots [16]. Heat is generated at the contact interfaces due to the contact resistances. In Joule heating systems, contact resistance heating can be substantial and needs to be taken into account.

168

169

170

In the towpregging line system, carbon fibre tow travelled over the roller electrodes and the current was transferred through the contact regions. The total resistance of the system can be defined as:

171

173

172

$$R_{total} = R_{CF} + R_{CR} + R_{cable} \quad (1)$$

174

175

176

177

178

179

180

181

182

183

184

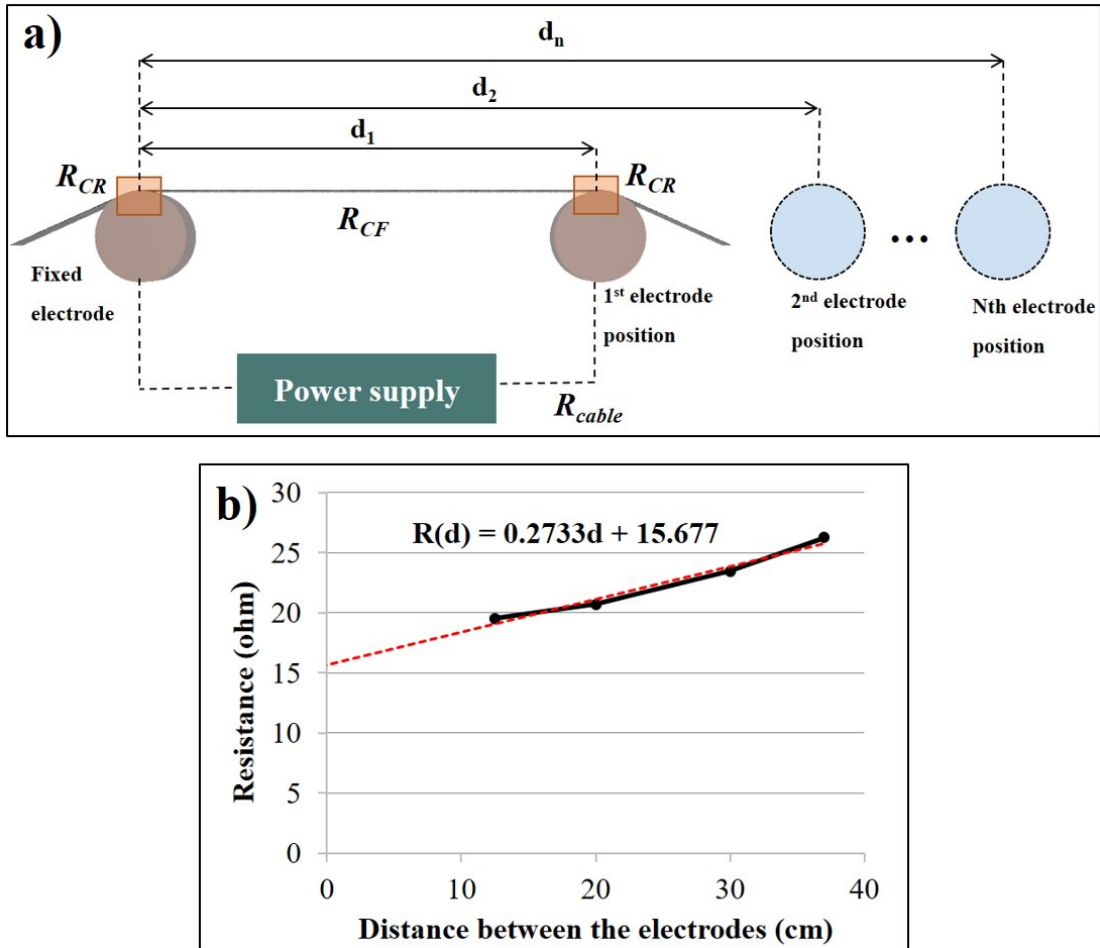
185

where  $R_{CF}$  is the carbon fibre resistance,  $R_{CR}$  is the contact resistances and  $R_{cable}$  is the resistance of the cables conducting current from the power supply to the electrodes ( $\Omega$ ). Assuming that material resistance changed linearly, the resistance of the entire system was measured for different distances between the electrodes (Figure 5a)). When the resistance values at different electrode distances  $R(d)$  were plotted, linear regression was used to find the y-intercept of the plot which yielded the contact resistance and the cable resistance (Figure 5b)). Finally, cable resistance was measured with a multimeter and subtracted from the value at y-intercept to calculate contact resistance values. Similar approaches were used to determine contact resistances in [9], [11], [18]. Carbon fibre has negative temperature coefficient (NTC) and Grohman [13] reported 2-3% drop in specific resistance for a temperature gradient of 100°C. Similarly, Forintos and Czigany [26] reported ~2.5% drop of resistance for carbon fibre that was heated from 20 to 120°C. However, for the sake of simplicity, the influence of NTC of the

186 carbon fibre on the contact resistances was neglected. Contact resistance values were measured  
 187 for different process parameters, such as tow tension, production speed and temperature.

188

189



190

191 **Figure 5:** (a) The methodology used to measure the contact resistance of the Joule  
 192 heating system and (b) sample dataset for linear regression.

193

194 **3. Results and Discussion**

195

196

3.1. Contact resistance values

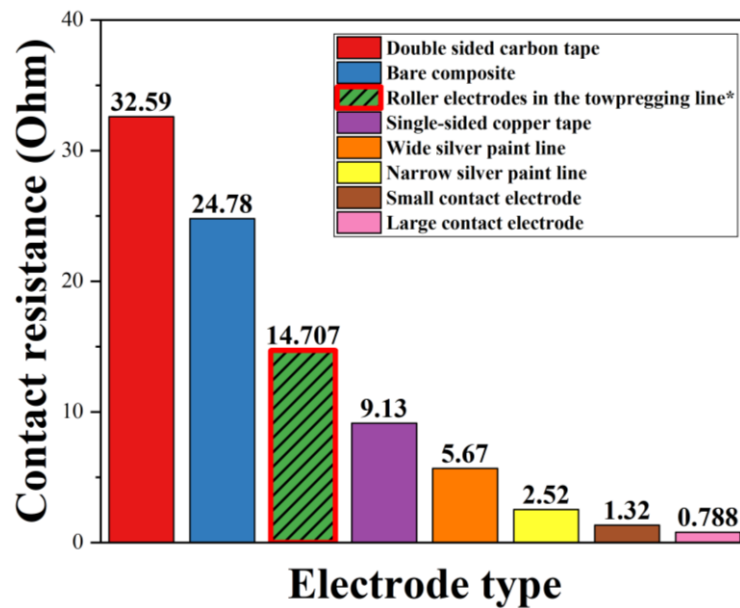
197 In most Joule heating systems of composite materials, electrodes and the composite material are  
 198 stationary [1], [2], [4], [5], [27]–[31]. In these systems, contact resistances can be reduced by  
 199 improving the contact interface, such as sanding the electrode/composite surfaces [9] or  
 200 applying silver paste [5], [27], [31]. However, the towpregging line is a dynamic system with  
 201 rotating roller electrodes and moving carbon fibre tow, which was designed to have high  
 202 production speeds (up to 30 m/min). As the carbon fibre tow and roller electrodes are in constant



203 motion, it is difficult to achieve the same level of contact that is possible with stationary Joule  
 204 heating systems using the aforementioned improvements. Therefore, the measured contact  
 205 resistance values were higher in the towpregging line (ranging between 10-20  $\Omega$ ) than similar  
 206 Joule heating systems which use methods to improve the interfaces. Kwok and Hahn [9]  
 207 demonstrated that the electrode type is crucial for good contact in Joule heating systems, they  
 208 found that resistivities between 0.788 and 32.59  $\Omega$  were possible depending on the electrode  
 209 type.

210 Figure 6 compares the values of contact resistances for different electrode types reported in [9]  
 211 and the measured values for the Joule heating section of the towpregging line at 5 m/min  
 212 production speed and 20 N tension. From this comparison, it can be inferred that the  
 213 tow/electrode coupling was inferior to the systems which used additional elements (silver paint,  
 214 clamps etc.) to abate contact resistances. Nevertheless, it exhibited lower values than simpler  
 215 systems such as double-sided carbon tape or alligator clips.

216 The contact between the carbon fibre tow and the roller electrodes in the towpregging line is  
 217 inherently imperfect, as the carbon fibre travels rapidly in the line during the production.  
 218 Depending on the production speed, the contact time between the carbon fibre tow and roller  
 219 electrodes occurs in only a fraction of a second. Moreover, the portion of the tow that is in  
 220 contact with the rollers changes constantly, and the packing of filaments rearranges, leading to  
 221 the changes in the contact area.



222  
 223 **Figure 6:** Comparison of contact resistances measured in the towpregging line (at 5 m/min  
 224 production speed and 20 N tension) and different electrode types reported by Kwok and Hahn  
 225 [9].

226  
 227 There is a significant relationship between the contact resistances and the contact area of the  
 228 interfaces. Mulvihill et al. [32] demonstrated that the real contact area between the carbon fibre  
 229 tows and a flat tool can be significantly lower than the nominal area. They reported that the real

230 contact area of carbon fibre tow on a flat tool could be as low as 0.4% of the nominal contact  
231 area. Furthermore, they concluded that highly sized carbon fibre tow T700SC-12K-50C (1%  
232 sizing), which is the same material used in this study except for the filament count, made less  
233 contact than lightly sized (0.3% sizing) tow. This was because a higher sizing ratio caused  
234 greater cohesion between fibres, which, consequently, led to stiffer tows. Thus, it can be inferred  
235 that the primary reason for the relatively high contact resistances in the towpregging line was  
236 the very low contact area between the heavily sized carbon fibre tow and the rough electrode  
237 surface.

238

### 239 3.2. Effect of tow tension

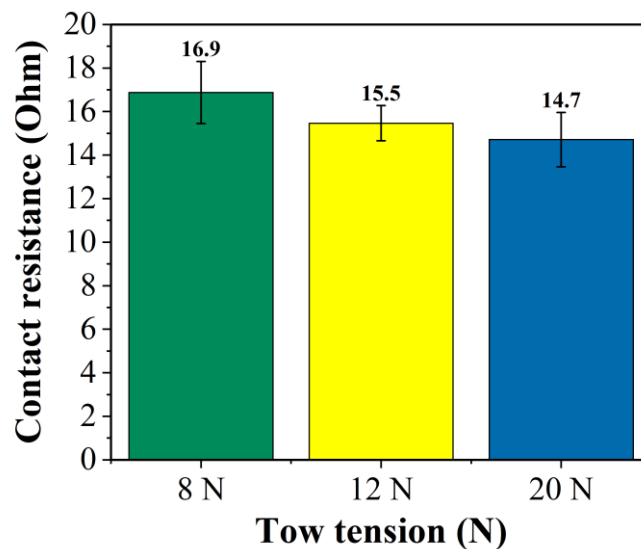
240

241 The carbon fibre tow in the towpregging line is under constant tension during the production. A  
242 PID controlled magnetic brake applies desired tension on the tow, and a tension sensor measures  
243 the tension of the tow. Tension applied on the tow ensures uniform heating and better  
244 consolidation of the molten powder-epoxy.

245

246 In order to evaluate the influence of tow tension on the contact resistances, 8, 12, and 20 N  
247 constant tension were applied to the tow during contact resistance measurements, as shown in  
248 Figure 7.

249



250

251 **Figure 7:** Effect of tow tension on the contact resistances at constant production speed (5  
252 m/min) and room temperature.

253

254 From Figure 7, it can be seen that the contact resistance of the system reduced with increased  
255 tow tension. At 5 m/min production speed, a value of  $16.9 \pm 1.43 \Omega$  was recorded at 8 N,  
256  $15.5 \pm 0.81 \Omega$  at 12 N and  $14.7 \pm 1.25 \Omega$  at 20 N. Contact resistance values calculated for higher

257 tension (20 N) were 12.6% smaller than for low tension (8 N), which indicated an enhanced  
258 contact with increased tension.

259  
260 In line with these results, Mulvihill et al. [32] reported that the true contact length of carbon  
261 fibre tows increased from 0.8% at 0.6 kPa to 25.9% at 305.5 kPa pressure, which emphasizes  
262 the importance of pressure (or tension) on the electrode/material interface. The tension of the  
263 tows increased the number of the carbon fibre filaments in contact with the electrode surface,  
264 as well as the length of filament contacts. Hence, the contact area increased, the current was less  
265 constrained and contact resistances dropped. Increased tension also aligns filaments better,  
266 reducing the number of filaments crossing over other filaments which reduces the contact area  
267 drastically [32].

268  
269

### 270 *3.3. Effect of production speed*

271 Higher production speeds in the towpregging line are required to reach industry-scale  
272 production. A speed sensor constantly measures the speed of the production and communicates  
273 with the PID controller, which changes collection reel motor voltage to control the speed. As it  
274 directly influences powder deposition, heating, and cooling of the towpreg, speed is one of the  
275 most important process parameters in the towpregging line.

276 At a constant tension of 8 N, the contact resistance of the Joule heating system was measured at  
277 3, 5, and 10 m/min production speeds to investigate the influence of speed on the contact  
278 interfaces. Figure 8 illustrates the change of contact resistance with speed: at 8 N tension, a  
279 value of  $14.9 \pm 0.61 \Omega$  was obtained at 3 m/min,  $16.9 \pm 1.43 \Omega$  at 5 m/min and  $18.1 \pm 1.15 \Omega$  at 10  
280 m/min. The same trend was observed at different tensions; contact resistances increased with  
281 production speed. The contact resistance of the system increased 21.3% when the production  
282 speed was increased from 3 to 10 m/min.

283 As the production speed increases, the tow travels faster in the line, and the duration of contact  
284 with the electrodes gets shorter. The tow travels 5 cm in a second when the production speed is  
285 3 m/min, but it travels 16.6 cm in a second if the production speed is increased to 10 m/min.  
286 Considering the diameter of the roller electrodes (2 cm), it is evident that the contact between  
287 the tow and the electrodes occurs only for a brief time. Despite the applied tension pressing the  
288 tow against the roller surface, at higher production speeds tow is unable to conform to the roller  
289 electrodes and the real contact area becomes even smaller. Moreover, there is less control over  
290 the process at higher speeds; hence it is likely that additional factors reduce the contact area,  
291 such as unaligned filaments or filaments crossing over the width of the tow.

292

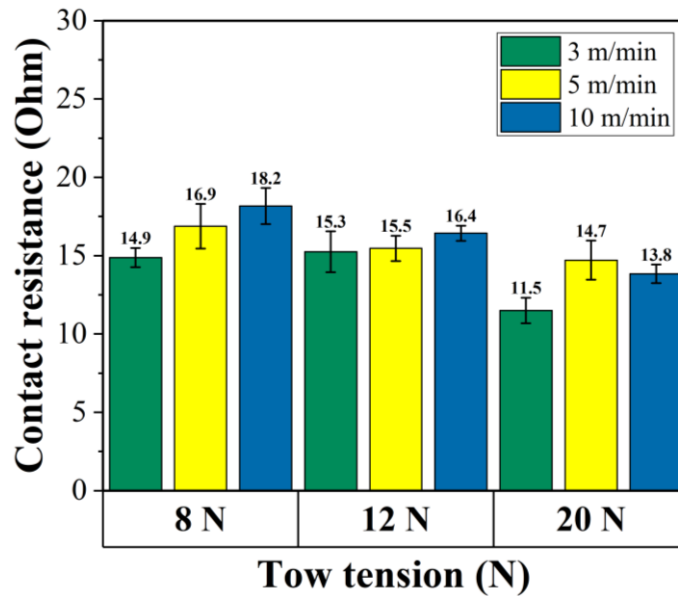
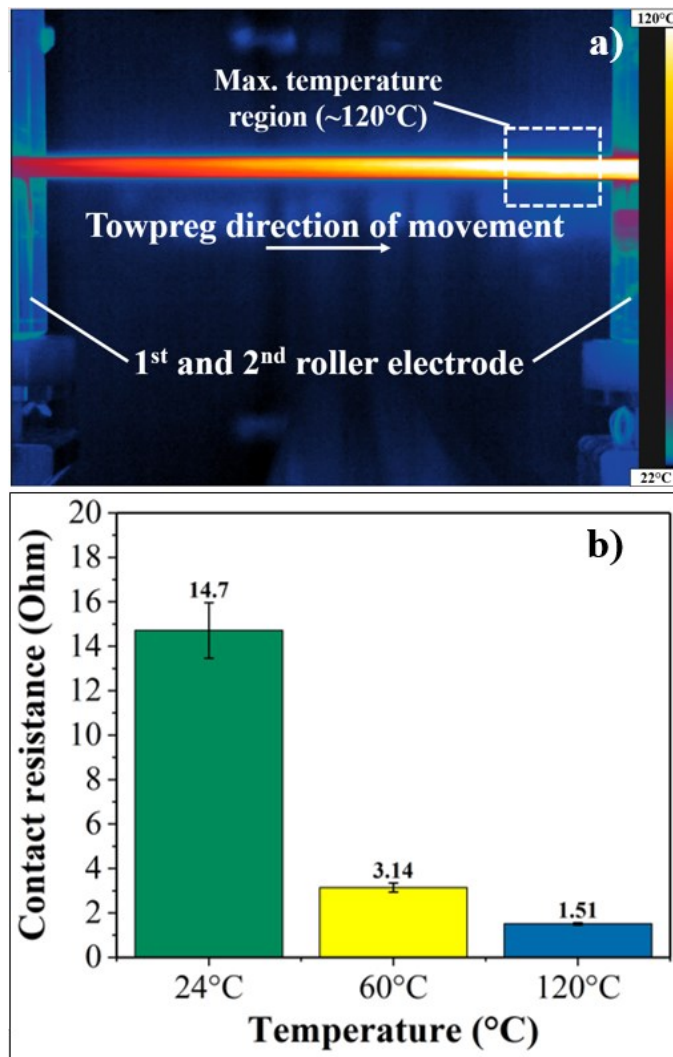


Figure 8: The effect of production speed at different tow tensions.

#### 3.4. Effect of temperature

The maximum temperature region shifted towards the direction of movement during the experiments (Figure 9a)). An infrared temperature sensor was positioned in this region to monitor the maximum temperature in the heating section.

For the same tension (20 N) and production speed (5 m/min), the maximum temperature of the heated section was set to 24°C, 60°C, and 120°C during contact resistance measurements (Figure 9b)). The temperature was found to have a significant impact on contact resistances, the measured contact resistance was 14.7±1.25 Ω at 24°C, 3.1±0.2 Ω at 60°C and 1.5±0.05 Ω at 120°C. The contact resistance value measured for 24°C is 89.7% greater than that of 120°C. Increased temperature enhanced the contact interface between the roller electrodes and the carbon fibre tow, and allowed the tow to conform to the electrode surfaces better due to its transverse thermal expansion. Although carbon fibres have negative longitudinal coefficient of thermal expansion, transverse coefficient of thermal expansion was reported to be much higher [33].



311

312

313

314

**Figure 9:** a) The shift of maximum temperature region towards towpreg direction of movement b) Effect of maximum temperature region on the contact resistance.

315

316

### 3.5. Contact resistive heating

317

318

319

320

321

322

323

324

325

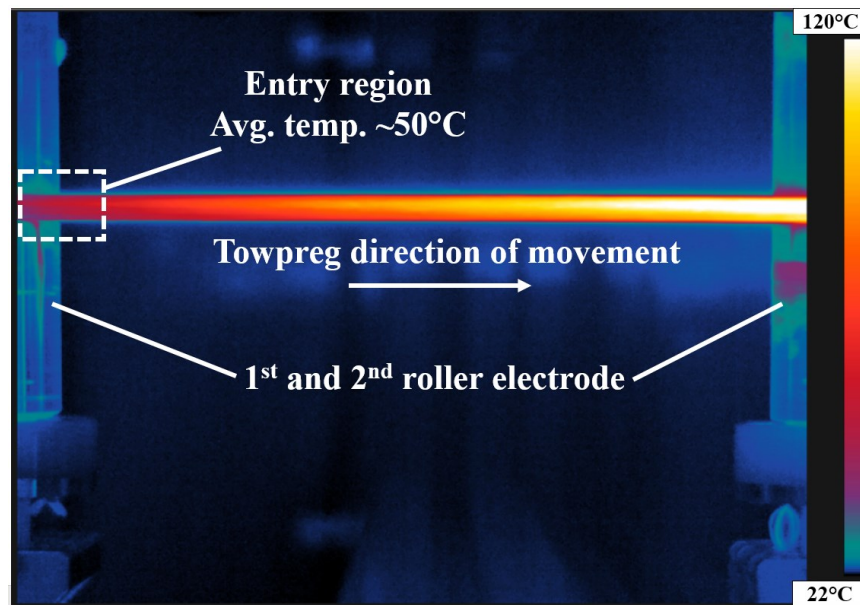
326

The heat generated at the tow-electrode interfaces due to contact resistances, as explained in Section 2.3., can be remarkably high. Sierakowski et al. [16] showed that contact resistance heating becomes far more significant than Joule heating when the current is supplied to the unidirectional composite plate for longer durations (>5 min). A thermal camera (FLIR A655SC) was used to visualize the contact resistance heating in the towpregging line. The thermal camera image presented in Figure 10 highlighted that the carbon fibre tow entered the Joule heating zone at an elevated temperature. This preheating of the tow was due to contact resistance heating at the interface of the first roller electrode. As such, Joule heating of the tow started at ~50°C, rather than ambient temperature, and then increased to a maximum temperature of ~120°C. Heat generated due to contact resistance was shared between the moving tow and the metal

327 roller electrodes. Roller electrodes have larger thermal capacity and higher thermal conductivity  
328 than the carbon fibre tow. Besides, due to the fact that rollers have fixed positions within the  
329 heating zone, whereas the carbon fibre tow passes through, it can be assumed most of the  
330 produced heat is accumulated in the metal roller electrodes, making the electrodes act as  
331 “preheaters” that provided additional conductive heating to the tow. If there was no contact  
332 resistance heating in the contact regions, the average temperature of the tow at the entry region  
333 would be around room temperature, and the heating of the first roller would be minimal (in  
334 actuality, the temperature of the first roller electrode reaches 30-35°C in a production run).

335 With a melt temperature of around 40°C [19], the powder melt phase change begins as soon as  
336 it enters the Joule heating section and completely melts before leaving the heating section. The  
337 contact resistance heating in the system might be actually beneficial in terms of providing a  
338 more uniform temperature distribution (i.e. less temperature difference) along the heating  
339 section. This would help the towpreg to reach the desired temperature at higher production  
340 speeds; in cases where the tow passes through the heated section too fast to be adequately  
341 subjected to the electric current. Furthermore, the heat stored in the roller electrodes helps  
342 reduce the powder agglomeration around the roller.

343



344

345 **Figure 10:** Thermal camera image from the top view of the Joule heating section.

346

### 347 3.6. Computational model

348 A simple finite element model was developed using COMSOL Multiphysics 5.6 software to  
349 examine the influence of contact resistance heating for the towpregging line. The model  
350 calculates the temperature distribution of the moving tow due to the power generated from the  
351 Joule heating and contact resistance heating separately. The heat produced by Joule heating in  
352 the carbon fibre tow  $Q_{JH}$  (W/m<sup>3</sup>) can be expressed by Eq. 2 [27]:

353

355

$$Q_{JH} = \frac{I^2}{\sigma V} \quad (2)$$

354

356

where  $I$  is the current passing through the carbon fibre (A),  $\sigma$  is the electrical conductivity of carbon fibre (S/m) and  $V$  is the volume of the heated section of carbon fibre ( $\text{m}^3$ ). The heat equation then can be rewritten as Eq. 3 [16]:

357

358

359

361

$$c\rho \frac{\partial T}{\partial t} = \nabla(\mathbf{k}\nabla T) + \frac{I^2}{\sigma V} \quad (3)$$

360

362

where  $c$  is the specific heat capacity (kJ/kg.K),  $\rho$  is the density ( $\text{kg}/\text{m}^3$ ),  $T$  is the temperature (K),  $t$  is the time (s) and  $\mathbf{k}$  is the thermal conductivity tensor of the carbon fibre tow (W/m K). Being a measure of material resistivity, the electrical conductivity of the carbon fibre tow  $\sigma$  is a key parameter for the Joule heating.

363

364

365

366

Heat is generated as a consequence of the contact resistances at the interfaces, which can be expressed as [14]:

367

368

370

$$Q_{CR} = \frac{I^2 R_{CR}}{A} \quad (4)$$

369

371

where  $Q_{CR}$  is the heat generated by the contact resistances ( $\text{W}/\text{m}^2$ ),  $I$  is the current (A),  $R_{CR}$  is the contact resistance ( $\Omega$ ) and  $A$  is the contact area of the interface ( $\text{m}^2$ ).

372

373

374

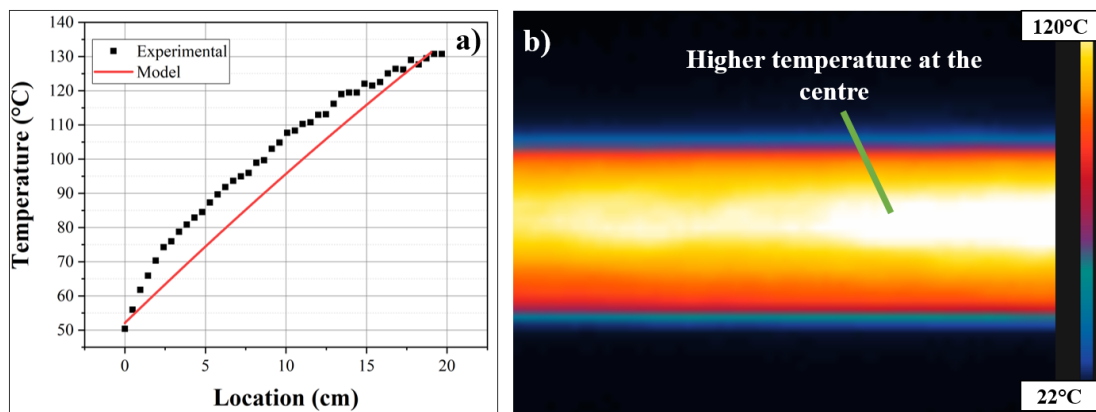
**Table 1:** Key model parameters

Parameter	Value
Width of the tow [mm]	6.35
Thickness of the tow [mm]	0.23
Length of heated section [mm]	190
Electrical conductivity of carbon fibre [S/m]	30960
Total contact resistance at 120°C [ $\Omega$ ]	1.5
Applied current [A]	2
Speed of the tow [m/min]	6.5
Thermal conductivity [W/m.K]	9.6
Density [ $\text{kg}/\text{m}^3$ ]	1800
Specific heat [J/kg.K]	752

375

376 Table 1 summarises key parameters that are used in the model. In the model, the effect of contact  
 377 resistance heating was taken into account by employing a thin layer of high resistance region  
 378 that produces the heat  $Q_{CR}$  at the contact interfaces. Figure 11a) illustrates the good agreement  
 379 of the temperature values along the moving tow from the model and experimental data, which  
 380 were captured by the thermal camera. However, due to the uneven tension across the width of  
 381 the tow, the temperature at the centre is slightly higher than the sides (Figure 11b)), therefore,  
 382 fluctuations and deviations are observed in the experimental data.

383



384

385 **Figure 11:** (a) Comparison of predicted temperature values by the model and experimental  
 386 measurements (b) local temperature variations due to the uneven tension profile across the width  
 387 of the tape

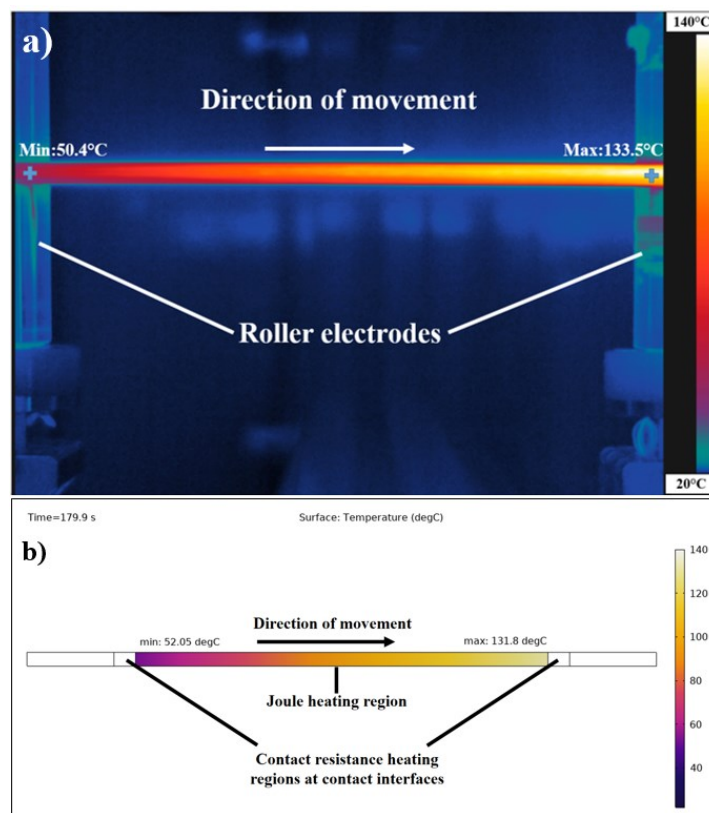
388

389 It is evident from experimental and modelling results that the temperature of the tow reaches  
 390  $\sim 50^\circ\text{C}$  at the beginning of the Joule heating zone (entry region), due to the contact resistance  
 391 heating occurring at the contact interfaces. This creates a more uniform temperature distribution  
 392 in the heated section of the tow; a smooth transition of the temperature from  $\sim 50^\circ\text{C}$  to  $\sim 135^\circ\text{C}$   
 393 can be observed in Figure 12. As mentioned before, the viscosity of the powder-epoxy is  
 394 minimum around  $120^\circ\text{C}$  and melting starts at  $\sim 40^\circ\text{C}$ . Therefore, powder melt can initiate even  
 395 from the entry region, thanks to contact resistance heating. The highest temperature in the tow  
 396 is not obtained at the centre of the heating zone, but it is towards the direction of movement  
 397 (near the second roller). It was observed that the maximum temperature reached does not change  
 398 significantly with contact resistance heating in transient conditions ( $< 5$  min), as it depends  
 399 heavily on the Joule heating rather than contact resistance heating, due to the much higher  
 400 energy. At high temperatures, the power drawn for the Joule heating system is also increased  
 401 and it dwarfs the effect of contact resistance heating. For the prolonged production runs, the first  
 402 roller temperature increases (up to  $40\text{-}50^\circ\text{C}$ ) and the conductive heat transfer from the roller to  
 403 the tow can also increase the temperature of the tow. However, it is difficult to observe this in  
 404 the maximum temperature region as the temperature is already high, but it is relatively easier to  
 405 detect it in the entry region where the temperature of the tow should be near room temperature.  
 406 Besides, heat transfer to the ambient via convection and radiation is also maximized near the  
 407 maximum temperature region, therefore the additional temperature from the contact resistance  
 408 heating might be outweighed.



409 As a result of using contact resistance data from the experiments, the model accuracy for the  
410 entry region was greatly improved. Having an accurate model for the temperature distribution  
411 of the tow not only provides a better understanding of the heating process, but also paves the  
412 way for further multiphysics models. By coupling the heat transfer model to an appropriate  
413 melting and sintering model, the melting behaviour of the powder can be analysed in detail,  
414 which is difficult experimentally. In addition, models for consolidation and flow of the molten  
415 powder within the tow requires the temperature distribution of the heating section of the line.  
416 Thus, improved model accuracy of the heat transfer model by accounting for contact resistances  
417 is beneficial for further process models of the towpregging line.

418



419

420 **Figure 12:** Temperature distribution of the tow captured by IR camera (a) and predicted by  
421 the model (b)

422

423

#### 424 4. Conclusions

425

426 Joule heating is a promising heating method for composite applications such as curing or self-  
427 healing. Low power consumption, uniform heating and inexpensive set-up are some of the  
428 advantages of Joule heating systems, however, contact resistances occurring at the interfaces  
429 between electrodes and the material play a key role in the heating behaviour. This present study  
430 investigated the role of contact resistances and contact resistance heating in a powder-epoxy  
431 based towpregging line, which employs Joule heating to heat carbon fibre tows. Contact  
432 resistance values in the heating system were measured for different process parameters, such as

433 tow tension, production speed and temperature for dry carbon fibre tows (i.e. powder was not  
434 deposited on the tows). It was found that process parameters change contact resistances  
435 considerably, and, hence, the overall heating performance within the towpregging line. Contact  
436 resistances increased with production speed and reduced with increased tow tension and higher  
437 temperatures. A thermal camera was used to analyse the effect of contact resistance heating on  
438 the system. Measured contact resistance values were used in a finite element model to obtain  
439 the temperature distribution along the carbon fibre tow. Thermal camera images and model  
440 results showed good agreement. The findings confirmed that contact resistances are significant  
441 in the system and alter the heating profile of the carbon fibre tows. Furthermore, measuring the  
442 contact resistance values provides valuable input for process models of the towpregging line.  
443

#### 444 **5. Acknowledgements**

445 This study was funded by CIMCOMP EPSRC Future Composites Manufacturing Research Hub  
446 (EP/P006701/1). The author wishes to express his thanks for the financial support of the Republic  
447 of Turkey Ministry of National Education Scholarship Program.

#### 448 **6. Disclosure**

449 The authors report there are no competing interests to declare.

#### 450 **7. References**

- 451 [1] T. Xia, D. Zeng, Z. Li, R. J. Young, C. Vallés, and I. A. Kinloch, “Electrically conductive  
452 GNP/epoxy composites for out-of-autoclave thermoset curing through Joule heating,” *Compos. Sci.*  
453 *Technol.*, vol. 164, pp. 304–312, Aug. 2018.
- 454 [2] C. Joseph and C. Viney, “Electrical resistance curing of carbon-fibre/epoxy composites,”  
455 *Compos. Sci. Technol.*, vol. 60, no. 2, pp. 315–319, Feb. 2000.
- 456 [3] B. Mas, J. P. Fernández-Blázquez, J. Duval, H. Bunyan, and J. J. Vilatela, “Thermoset curing  
457 through Joule heating of nanocarbons for composite manufacture, repair and soldering,” *Carbon N. Y.*,  
458 vol. 63, pp. 523–529, Nov. 2013.
- 459 [4] S. Gómez-Barreiro, C. Gracia-Fernández, J. López-Beceiro, and R. Artiaga, “Rheological  
460 testing of a curing process controlled by Joule heating,” *Polym. Test.*, vol. 55, pp. 97–100, Oct. 2016.
- 461 [5] X. Xu, Y. Zhang, J. Jiang, H. Wang, X. Zhao, Q. Li and W. Lu, “In-situ curing of glass fiber  
462 reinforced polymer composites via resistive heating of carbon nanotube films,” *Compos. Sci. Technol.*,  
463 vol. 149, pp. 20–27, Sep. 2017.
- 464 [6] B. Shi, Y. Shang, P. Zhang, S. Liu, S. Huang, B. Sun, B. Gu, and K. Fu, “Rapid electrothermal-  
465 triggered flooded thermoset curing for scalable carbon/polymer composite manufacturing,” *Compos.*  
466 *Sci. Technol.*, vol. 200, p. 108409, Nov. 2020.
- 467 [7] J. Reese, G. Hoffmann, J. Fieres, and C. Cherif, “Characterization of the electrical behavior of  
468 a discontinuous hybrid yarn textile made of recycled carbon and PA6 fibers during Joule heating,” *J.*  
469 *Thermoplast. Compos. Mater.*, vol. 2020, no. 10, pp. 1317–1335.
- 470 [8] J. Orellana, I. Moreno-Villoslada, R. K. Bose, F. Picchioni, M. E. Flores, and R. Araya-  
471 Herмосilla, “Self-Healing Polymer Nanocomposite Materials by Joule Effect,” *Polym.* 2021, Vol. 13,  
472 Page 649, vol. 13, no. 4, p. 649, Feb. 2021.

- 475 [9] N. Kwok and H. T. Hahn, "Resistance Heating for Self-healing Composites:," *J. Compos.*  
476 *Mater.*, vol. 41, no. 13, pp. 1635–1654, Jul. 2007.
- 477 [10] Q. OuYang, X. Wang, and L. Liu, "High crack self-healing efficiency and enhanced free-edge  
478 delamination resistance of carbon fibrous composites with hierarchical interleaves," *Compos. Sci.*  
479 *Technol.*, vol. 217, p. 109115, Jan. 2022.
- 480 [11] S. J. Joo, M. H. Yu, W. S. Kim, and H. S. Kim, "Damage detection and self-healing of carbon  
481 fiber polypropylene (CFPP)/carbon nanotube (CNT) nano-composite via addressable conducting  
482 network," *Compos. Sci. Technol.*, vol. 167, pp. 62–70, Oct. 2018.
- 483 [12] S. A. Hayes, A. D. Lafferty, G. Altinkurt, P. R. Wilson, M. Collinson, and P. Duchene, "Direct  
484 electrical cure of carbon fiber composites," *Adv. Manuf. Polym. Compos. Sci.*, vol. 1, no. 2, pp. 112–  
485 119, Apr. 2015.
- 486 [13] Y. Grohmann, "Continuous Resistance Heating Technology for High-Speed Carbon Fibre  
487 Placement Processes," in *SAMPE Europe 2020*, 2020, pp. 3–12.
- 488 [14] A. E. Zantout and O. I. Zhupanska, "On the electrical resistance of carbon fiber polymer matrix  
489 composites," *Compos. Part A Appl. Sci. Manuf.*, vol. 41, no. 11, pp. 1719–1727, Nov. 2010.
- 490 [15] M. Hamed and M. Atashparva, "A review of electrical contact resistance modeling in resistance  
491 spot welding," *Weld. World*, vol. 61, no. 2, pp. 269–290, Mar. 2017.
- 492 [16] R. L. Sierakowski, I. Y. Telitchev, and O. I. Zhupanska, "On the impact response of electrified  
493 carbon fiber polymer matrix composites: Effects of electric current intensity and duration," *Compos.*  
494 *Sci. Technol.*, vol. 68, no. 3–4, pp. 639–649, Mar. 2008.
- 495 [17] X. Qi, S. Zhu, H. Ding, and M. Xu, "Theoretical and experimental analysis of electric contact  
496 surface hardening of ductile iron," *Appl. Surf. Sci.*, vol. 288, pp. 591–598, Jan. 2014.
- 497 [18] E. B. Jeon, T. Fujimura, K. Takahashi, and H. S. Kim, "An investigation of contact resistance  
498 between carbon fiber/epoxy composite laminate and printed silver electrode for damage monitoring,"  
499 *Compos. Part A Appl. Sci. Manuf.*, vol. 66, pp. 193–200, Nov. 2014.
- 500 [19] C. Robert, T. Pecur, J. M. Maguire, A. D. Lafferty, E. D. McCarthy, and C. M. Ó. Brádaigh, "A  
501 novel powder-epoxy towpregging line for wind and tidal turbine blades," *Compos. Part B Eng.*, vol.  
502 203, p. 108443, Dec. 2020.
- 503 [20] J. M. Maguire, K. Nayak, and C. M. Ó Brádaigh, "Characterisation of epoxy powders for  
504 processing thick-section composite structures," *Mater. Des.*, vol. 139, pp. 112–121, Feb. 2018.
- 505 [21] J. M. Maguire, P. Simacek, S. G. Advani, and C. M. Ó Brádaigh, "Novel epoxy powder for  
506 manufacturing thick-section composite parts under vacuum-bag-only conditions. Part I: Through-  
507 thickness process modelling," *Compos. Part A Appl. Sci. Manuf.*, vol. 136, p. 105969, Sep. 2020.
- 508 [22] M. Çelik, T. Noble, F. Jorge, R. Jian, C. M. Ó. Brádaigh, and C. Robert, "Influence of Line  
509 Processing Parameters on Properties of Carbon Fibre Epoxy Towpreg," *J. Compos. Sci.* 2022, Vol. 6,  
510 Page 75, vol. 6, no. 3, p. 75, Mar. 2022.
- 511 [23] D. Mamalis, T. Flanagan, and C. M. Ó Brádaigh, "Effect of fibre straightness and sizing in  
512 carbon fibre reinforced powder epoxy composites," *Compos. Part A Appl. Sci. Manuf.*, vol. 110, pp.  
513 93–105, Jul. 2018.

- 514 [24] Chemours, “Tefzel ETFE HT-2170 Fluoropolymer Resin”, K-27427 datasheet, 2016.
- 515 [25] Chemours, “Teflon PFA C-980 Fluoroplastic Resin”, K-27853 datasheet, 2018.
- 516 [26] N. Forintos and T. Czigany, “Reinforcing carbon fibers as sensors: The effect of temperature  
517 and humidity,” *Compos. Part A Appl. Sci. Manuf.*, vol. 131, p. 105819, Apr. 2020.
- 518 [27] M. Lu, J. Xu, P. J. Arias-Monje, P. V. Gulgunje, K. Gupta, N. Shirolkar, A. P. Maffe, E.  
519 DiLoreto, J. Ramadachandran, Y. Sahoo, S. Agarwal, C. Meredith and S. Kumar, “Continuous  
520 stabilization of polyacrylonitrile (PAN) - carbon nanotube (CNT) fibers by Joule heating,” *Chem. Eng.  
521 Sci.*, vol. 236, p. 116495, Jun. 2021.
- 522 [28] J. Seyyed Monfared Zanjani, B. Saner Okan, P. N. Pappas, C. Galiotis, Y. Z. Menciloglu, and  
523 M. Yildiz, “Tailoring viscoelastic response, self-heating and deicing properties of carbon-fiber  
524 reinforced epoxy composites by graphene modification,” *Compos. Part A Appl. Sci. Manuf.*, vol. 106,  
525 pp. 1–10, Mar. 2018.
- 526 [29] V. Baheti and Y. Wang, “Ohmic heating and mechanical stability of carbon fabric/green epoxy  
527 composites after incorporation of fly ash particles,” *Mater. Today Commun.*, vol. 26, p. 101710, Mar.  
528 2020.
- 529 [30] Y. G. Jeong and J. E. An, “Effects of mixed carbon filler composition on electric heating  
530 behavior of thermally-cured epoxy-based composite films,” *Compos. Part A Appl. Sci. Manuf.*, vol. 56,  
531 pp. 1–7, Jan. 2014.
- 532 [31] A. T. Chien, S. Cho, Y. Joshi, and S. Kumar, “Electrical conductivity and Joule heating of  
533 polyacrylonitrile/carbon nanotube composite fibers,” *Polymer (Guildf.)*, vol. 55, no. 26, pp. 6896–6905,  
534 Dec. 2014.
- 535 [32] D. M. Mulvihill, O. Smerdova, and M. P. F. Sutcliffe, “Friction of carbon fibre tows,” *Compos.  
536 Part A Appl. Sci. Manuf.*, vol. 93, pp. 185–198, Feb. 2017.
- 537 [33] R. Kulkarni and O. Ochoa, “Transverse and Longitudinal CTE Measurements of Carbon Fibers  
538 and their Impact on Interfacial Residual Stresses in Composites:,” *J. Compos. Mater.*, vol. 40, no. 8, pp.  
539 733–754, Jul. 2005.
- 540